Optimization of heterogeneous arrays of wave energy converters

Habeebullah Abdulkadir[a], Ossama Abdelkhalik[a,*]

[a]Department of Aerospace Engineering, Iowa State University, Ames, IA 50010, USA,

ARTICLE INFO

Keywords:
Wave energy converter
Layout Optimization
Size optimization
Homogeneous array
Heterogeneous array
Optimal control
Semi-analytic hydrodynamics.

ABSTRACT

Optimizing the layout of devices in an array of wave energy converters (WECs) is one of the core aspects of WEC array design. More often than not, WEC arrays are designed to contain identical devices. However, to further improve power generation, this paper investigates how devices of varying dimensions can affect the overall performance of the array; the array containing devices of different sizes is referred to as a heterogeneous array in this work. The heterogeneity is achieved by varying the radius and draught of cylindrical buoys. We measured the performance of the heterogeneous array against the homogeneous array containing the same number of devices in an identical layout, assuming the summation of volumes of all devices is the same for both the heterogeneous and the homogeneous arrays. The power from the array is computed using a time-domain array dynamic model and an optimal constrained control. The hydrodynamic coefficients used as input in the dynamic model are computed using a semi-analytical method to enable computationally efficient optimization. The optimization was performed using a genetic algorithm. Several case studies are presented. Heterogeneous arrays were found to perform better than homogeneous arrays.

1. Introduction

In recent decades, the global energy requirement increased as the human population continues to grow. According to the International Energy Outlook 2021 (IEO2021), global energy consumption is projected to increase by nearly 50% over the next 30 years (Zhongming, Linong, Xiaona, Wangqiang, Wei et al., 2021). Renewable energy sources, which include solar and wind, are projected to grow to nearly the same level as fossil fuel and other non-renewable sources in 2050. However, the continued development of efficient energy harvesting devices is an essential requirement for cutting down the cost of clean energy (Olabi and Abdelkareem, 2022; Nyangchak, 2022).

Compared to tidal energy, wave energy is the more significant form of ocean energy (de O. Falcao, 2010; Antonio, 2010; Cruz, 2007). WECs are used to harvest ocean wave energy. WECs are often categorized based on their mode of operation as: oscillating water column devices (Falcão and Henriques, 2016; Nagata, Toyota, Yasutaka, Setoguchi, Kyozuka and Masuda, 2007), overtopping converters (Drew, Plummer and Sahinkaya, 2009; Kofoed, Frigaard, Friis-Madsen and Sørensen, 2006) and point absorbers (Brekken, 2011; Pastor and Liu, 2014). The type of device considered in this work is a point absorber; they are characterized as having smaller dimensions compared to the wave length of the exciting wave.

The economic viability of WECs depends mainly on being scalable to add to a grid significantly. This will only be achieved by deploying many devices in an array. Reduction in installation, operation, and maintenance costs is another advantage of deploying multiple WECs in an array. However, a complex hydrodynamic interaction effect results from multiple devices being in close proximity. This interaction is not inherently bad; actually, it could be of advantage to array performance. This hydrodynamic interaction between devices in an array has been studied for years. Budal (1977) is often credited as the originator of wave energy device arrays study, pioneering the study of wave power absorption by interacting bodies within the context of linear theory. Child and Venugopal (2010b) investigated the influence of the spatial configuration of a wave energy device array upon total power using two approaches: a heuristic technique called the Parabolic Intersection (PI) method, and a Genetic Algorithm (GA). The GA produced better result, with the only downside found to be its computational requirement. The performance of a layout is measured using the q-factor; a ratio of the power from an array of N WEC devices to the power generated by the same N WECs when operating in isolation.

$$q = \frac{\boldsymbol{P}_{array}}{N\,\boldsymbol{P}_{isolated}} \tag{1}$$

In (Ruiz, Nava, Topper, Minguela, Ferri and Kofoed, 2017), the number of WECs in the array is considered a variable in a layout optimization problem. Three different optimization algorithms were compared. Neshat, Alexander, Sergiienko and Wagner (2019) explored algorithmic solutions to the problem of placing fully submerged spherical WECs buoys in arrays; nine new search heuristics to a range of existing standard and domain-specific search techniques were developed, evaluated and systematically compared. In (Snyder, Moarefdoost et al., 2014), master locations for different WEC numbers were found using point absorber approximation. The optimized locations arrays containing 2-15 devices were found, normalized by the wave number. Babarit (2010); Wolgamot, Taylor and Taylor (2012) studied

*This paper is based upon work supported by NSF, Grant Number 2048413. The research reported in this paper is partially supported by the HPC@ISU equipment at Iowa State University, some of which has been purchased through funding provided by NSF under MRI grant number 1726447.

*Ossama Abdelkhalik
https://www.aere.iastate.edu/ossama/ (Ossama Abdelkhalik)
ORCID(s):

the effects of wave direction on the array performance. De Andrés, Guanche, Meneses, Vidal and Losada (2014) ran time domain simulations to study the factors that influence array layout on wave energy farms in irregular waves. Factors analyzed in the paper are array layout, WEC separation, number of WECs and wave direction. Different layouts (linear, square and rhombus), WEC separation distances and incident wave directions are considered to assess the effect of design parameters on array power production for different Italian locations in (Bozzi, Giassi, Miquel, Antonini, Bizzozero, Gruosso, Archetti and Passoni, 2017).

Although optimization for the layout that maximized the positive interaction between the devices is the most common WEC array optimization problem in literature, other works have looked at other aspects of the WEC array problem. Lyu, Abdelkhalik and Gauchia (2019) investigated arrays of individually optimized dimensions, the radius of each cylindrical buoy is the optimization variable while the volume of the individual device is constrained. The performance measure used in the study was the q-factor, therefore, no comparison between the performance of the optimized heterogeneous array was made to a counterpart homogeneous array. Göteman, Engström, Eriksson and Isberg (2015) investigated the use of different WEC sizes and park geometries to minimize power fluctuations.

WEC array optimization problems are often computationally expensive; this is due to the fact that each solution considered during the optimization process requires calculating new sets of hydrodynamic coefficients of that particular solution under consideration. There are several methods used in computing the hydrodynamic coefficients of devices presented in literature, the first being the numerical boundary element (BEM) routines such as NEMOH (Babarit and Delhommeau, 2015), ANSYS Aqwa (ANSYS, 2013) and WAMIT (WAMIT User Manual, 2013). The computational cost when using this method, however, grows significantly as the number of WECs in the array increases. Another method for computing the hydrodynamic coefficients is the analytic point absorber approximation; the method assumes that the devices are small enough with respect to the wavelength of incident waves that the scattered waves can be neglected (Thomas and Evans, 1981; Falnes, 1980). A Semi-analytic approach that is based on a multiple scattering method is presented in (Kagemoto and Yue, 1993; Siddorn and Taylor, 2008; McIver, 2002). This semi-analytic approach can accurately compute the hydrodynamic coefficients assuming potential flow. The low computational cost of this semi-analytic approach has endeared it for use in WEC array optimization problems.

The hallmark of this work is investigating the performance of a heterogeneous WECs array compared to an array of optimized identical devices. An essential component of the current optimization involves choosing a device layout; optimal layouts are adapted from (Moarefdoost, Snyder and Alnajjab, 2017; Snyder et al., 2014) in this study. The adopted layouts are all symmetric along the exciting wave direction (x-axis). The optimization studies in this paper address two main objectives:

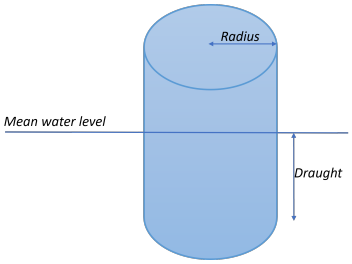

Figure 1: Cylindrical device.

1. Parameter optimization (radius and draught (Fig. 1)) of a device that maximizes the constructive interference in array of homogeneous devices.
2. Heterogeneous optimization of dimensions of individual devices that seek to achieve better interaction factor than the optimized homogeneous array.

In this study, the total volume of the heterogeneous array is constrained to being equal to the total volume of the optimized homogeneous array, within some error tolerance, to have a fair comparison. The remainder of this paper is organized as follows. In section II, the dynamic model and power principles for arrays of WECs is presented. Semi-analytic hydrodynamic computation method and its validation is presented in Section III. Section IV includes the optimization problem formulations. Simulations and results are discussed in section V. Conclusions are presented in Section VI.

2. WEC array dynamic model

The dynamic model for a single floating device can be represented as a second order mass-spring-damper system (Cummins). In frequency domain, dynamic equation for an array of heaving devices is written as (Falnes, 1999):

$$-\omega^2(\boldsymbol{M}+\boldsymbol{A})\vec{\mathbb{Z}}+j\omega(\boldsymbol{B_{PTO}}+\boldsymbol{B_r})\vec{\mathbb{Z}}+\boldsymbol{K_h}\vec{\mathbb{Z}}=\vec{\mathbb{F}}_{ex} \quad (2)$$

where $\boldsymbol{M}$ and $\boldsymbol{A}$ are the mass and hydrodynamic added mass matrices of the array, $\boldsymbol{B_{PTO}}$ and $\boldsymbol{B_r}$ are the PTO and radiation damping matrices, $\boldsymbol{K_h}$ is the hydrostatic coefficient matrix of the array, $\vec{\mathbb{Z}}$ is the heave displacement vector of the devices in the array and $\vec{\mathbb{F}}_{ex}$ is the heave wave excitation force. $\boldsymbol{A}$, $\boldsymbol{B_r}$ and $\vec{\mathbb{F}}_{ex}$ are the hydrodynamic coefficients; they are functions of device geometry, size, and the exciting wave frequency. These hydrodynamic coefficients can be calculated for using BEM routines such as NEMOH, ANSYS Aqwa and WAMIT or by alternative analytic and semi-analytic methods as discussed in section. 1.

The performance of an array during optimization is often assessed with frequency domain models. The average power absorbed by all devices in the array in a regular wave of unit amplitude using the derivative control can be calculated as:

$$\boldsymbol{P}(\beta,\omega) = \frac{\omega^2}{2}\vec{\mathbb{Z}}^T(\beta,\omega)\boldsymbol{B}_{PTO}\vec{\mathbb{Z}}(\beta,\omega) \tag{3}$$

where ω is the exciting wave frequency, β is the wave incidence angle, and $\vec{\mathbb{Z}}$ is the complex displacement vector of array solved from Eq. (2). According to (Falnes and Hals, 2012), the optimal power from the devices in the array can be harvested when the impedance of the system is matched. The optimum power is computed as:

$$\boldsymbol{P} = \frac{1}{8}\vec{\mathbb{F}}^*_{ex}\boldsymbol{B}_{\boldsymbol{r}}^{-1}\vec{\mathbb{F}}_{ex} \tag{4}$$

where $\vec{\mathbb{F}}_{ex}$ is the hydrodynamic excitation force, and $\vec{\mathbb{F}}^*_{ex}$ is its conjugate. The power evaluated by Eq. (4) is often found to significantly overestimate the absorbed power (Sergiienko, Neshat, da Silva, Alexander and Wagner, 2020), while the average absorbed power from Eq. (3) often yield sub-optimal results. A time-domain formulation is required for optimal performance of the WECs subject to system limitations. In recent years, multiple optimal and realistic controls have been proposed to achieve energy harvesting maximization; the control solution is computed by formulating the problem as a constrained optimization problem (Hals, Falnes and Moan, 2011; Li, Weiss, Mueller, Townley and Belmont, 2012; Bacelli and Ringwood, 2013; Zou, Abdelkhalik, Robinett, Bacelli and Wilson, 2017). An optimal power-constrained Bang-Singular-Bang (PCBSB) control formulation developed by the authors in (Abdulkadir and Abdelkhalik, 2022) maximizes the power extracted from an array of heaving WECs. The PCBSB control formulation accounts for the interaction between the devices in the array subject to control force and reactive power constraints. The time domain equivalent of the WEC array dynamics in Eq. (2) can be written in as:

$$(\boldsymbol{M}+\boldsymbol{A})\ddot{\vec{x}} = \vec{f}_e - \boldsymbol{B}_{\boldsymbol{r}}\dot{\vec{x}} - \boldsymbol{K}_{\boldsymbol{h}}\vec{x} - \vec{u} \tag{5}$$

where $\vec{x}$, $\dot{\vec{x}}$ and $\ddot{\vec{x}}$ are the position, velocity, and acceleration vectors of the N devices in the array. An analytic solution for the optimal control was found using Pontryagin's Minimum Principle as:

$$\vec{u}_{sa} = \vec{f}_e - \boldsymbol{B}_{\boldsymbol{r}}\dot{\vec{x}} - \boldsymbol{K}\vec{x} - [\boldsymbol{B}_{\boldsymbol{r}}[\boldsymbol{M}+\boldsymbol{A}]^{-1}]^{-1}\frac{\partial \vec{f}_e(t)}{\partial t} \tag{6}$$

The sequence of the optimal PCBSB control formulation is presented in Algorithm 1. The singular arc solution in Eq. (6) is saturated using a set maximum available control force limit, $\vec{\Upsilon}$, when the force constraint is violated and combined with a bang-bang control when the power constraint is violated. The PCBSB control has been implemented on an array of WECs and outperforms the optimal damping control.

Algorithm 1 PPBSB control Algorithm for a WEC array

procedure IMPLEMENT CONTROL FOR AN ARRAY OF DEVICES($\vec{u}$)
  Input: Maximum control force $\vec{\Upsilon}$,
  Output: Control
  Calculate excitation wave for the current time
  Compute singular arc control
  $\vec{u} = \vec{u}_{sa}$
  if $\vec{u}_{sa} \geq \vec{\Upsilon}$ **then**
    $\vec{u}_{sa} = \vec{\Upsilon}$
  else
    if $\vec{u}_{sa} \leq -\vec{\Upsilon}$ **then**
      $\vec{u}_{sa} = -\vec{\Upsilon}$
  Check power constraint.
  if $\vec{u}(t) \circ \dot{\vec{x}} < \vec{0}$ **then**
    $\vec{u} = sign(\dot{\vec{x}}) \times \vec{\Upsilon}$

3. Hydrodynamics coefficients computation

The mathematical theory and the modeling methodology for an array of interacting WEC array is presented in this section. The semi-analytical method used to compute the hydrodynamic coefficients used in the optimization problem is summarized. The formulations presented here follow the works on hydrodynamic interaction between multiple floating cylinders in waves by (Ohkusu, 1969; Matsui and Tamaki, 1981; Yilmaz, 1998; McNatt, Venugopal and Forehand, 2015; Child and Venugopal, 2010a). The computed coefficients is validated using results obtained from NEMOH BEM solver.

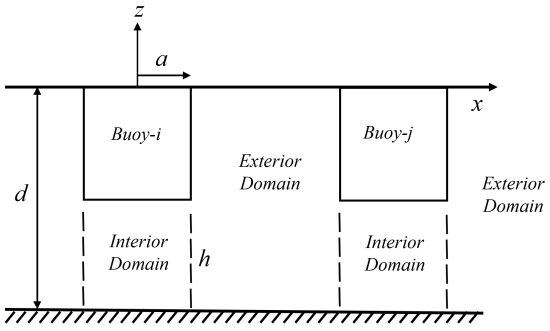

Figure 2: Fluid domains.

On the assumption of linear wave theory, i.e., incompressible, inviscid, and irrotational flow. Throughout the fluid, the velocity potential is described using a complex representation as:

$$\Phi(r,\theta,z,t) = Re\{\phi(r,\theta,z)\}e^{-i\omega t} \tag{7}$$

where $Re\{\}$ denotes the real part of the complex expression, ω is the angular frequency, and t is the time dependency. To be a valid solution, the spatial velocity potential $\phi(r,\theta,z)$ must satisfy the Laplace equation, and the linearised boundary conditions:

- The governing equation

$$\nabla^2\phi = 0 \tag{8}$$

- Free surface boundary conditions

$$\omega^2\phi - g\frac{\partial\phi}{\partial z}\Big|_{z=0} = 0 \tag{9}$$

- Sea bed condition

$$\frac{\partial\phi}{\partial z}\Big|_{z=-d} = 0 \tag{10}$$

- Impermeable surface condition on the body surface

$$\frac{\partial\phi}{\partial r} = 0,\ (r = a, -h \le z \le 0) \tag{11}$$

$$\frac{\partial\phi}{\partial z} = 0,\ (0 \le r \le a, z = -h) \tag{12}$$

- Cylinder body surface condition

$$\nabla\phi.\vec{n} = \vec{U}.\vec{n} \tag{13}$$

where $\vec{n}$ is the unit normal vector on the submerged surface and $\vec{U}$ is the body velocity. The Sommerfield radiation condition which must be satisfied by ϕ:

$$\lim_{x\to\infty}\sqrt{r}\left(\frac{\partial\phi}{\partial r} - ik_n\phi\right) = 0 \tag{14}$$

where k_n is the wave number solved from the dispersion relation given as:

$$\omega^2 = gktanh(kd) \tag{15}$$

the positive real solution, which is here denoted as k_0, is the wavenumber of the progressive mode. The negative imaginary solutions, k_n, for $n = 1, 2, ...$; are the wavenumbers of the evanescent modes.

The fluid region will be separated to the interior and exterior regions; the interior region being the region below the cylinders. $\phi^I(r, z)$ represents the spatial potential function of the flow in the interior region ($r \le a$) below the cylinder ($-h \le z \le -d$), while $\phi^E(r, z)$ is the potential of exterior region ($r \ge a$) outside of the cylinder ($0 \le z \le -d$). The overall velocity potential of the whole fluid domain can be broken down as;

$$\phi(r,\theta,z) = \phi_0(r,\theta,z) + \phi_7(r,\theta,z) + \sum_{q=1}^{6}\phi_q(r,\theta,z) \tag{16}$$

where ϕ_0 is the incident waves potential, ϕ_7 is the diffracted potential, ϕ_q and is the radiated potential due to the motion of the body in the direction , $q = 1, 3, 5$ corresponding to surge, heave, and pitch mode of motion, respectively.

3.1. Radiation problem

The radiation problem corresponds to the case where the cylinder is placed in calm water with no exciting wave, then forced to oscillate. The total radiation potential:

$$\phi_q(r,\theta,z) = \sum_{m=-\infty}^{\infty} i\omega H\varphi_{q,m}(r,z)cos(m\theta) \tag{17}$$

where H is the complex amplitude corresponding to the motion mode. In heaving mode ($q = 3$), and only expressions for $m = 0$ gave a contribution. We are then looking for solutions that can be expressed as:

$$\varphi_{3,m}(r,z) = \varphi_{3,h} + \varphi_{3,p} \tag{18}$$

where $\varphi_{3,p}$ represents a particular solution of the velocity potential in heave mode and $\varphi_{3,h}$ is the homogeneous part of the solution to the boundary value problem. The corresponding potential function for each region can be broken down as follows.

3.1.1. Interior region

The homogeneous potential for the interior region is given as:

$$\varphi^I_{3,h} = \frac{C_{R0}}{2}\left(\frac{r}{a}\right)^m + \sum_{n=1}^{\infty} C_{Rn}\frac{I_m(\frac{n\pi r}{(d-h)})}{I_m(\frac{n\pi a}{(d-h)})}cos(\frac{n\pi z}{(d-h)}) \tag{19}$$

The particular solution for an interior is given as:

$$\varphi^I_{3,p} = \frac{1}{2(d-h)}\left[(z+d)^2 - \frac{r^2}{2}\right] \tag{20}$$

where C_{Rn} are unknown fourier coefficients and I_m is the modified Bessel function of the first kind order m.

3.1.2. Exterior region

The homogeneous solution of the exterior radiation problem is given as:

$$\varphi^E_{3,h} = D_{R0}\frac{H_m(k_0r)}{H_m(k_0a)}Z_0(z) + \sum_{q=1}^{\infty} D_{Rq}\frac{K_m(k_qr)}{K_m(k_qa)}Z_n(z) \tag{21}$$

where D_{Rq} are unknown Fourier coefficients. H_m is Hankel function, and K_m is the modified Bessel function of the second kind, both of order m. $Z_q(z)$ is the depth dependency function. The depth dependency function $Z_q(z)$ is normalized to form an orthonormal set of eigenfunctions in the corresponding domain:

$$< Z_n(z), Z_q(z) >= \delta_{nq} \tag{22}$$

where δ_{nq} is the Kronecker delta.

3.2. Diffraction problem

The diffraction problem is the solution to the scattering of a fixed cylinder in the presence of an incident wave. The incident wave potential is defined as:

$$\phi_0(r,\theta,z) = \frac{gH}{\omega}\frac{cosh(k_0(z+d))}{coshk_0d}\sum_{m=-\infty}^{\infty} e^{im(\frac{\pi}{2}-\theta)}J_m(k_0r)e^{i\omega t} \tag{23}$$

3.2.1. Interior domain

The homogeneous solution is given as:

$$\varphi^I_{3,h} = \frac{C_0}{2}\left(\frac{r}{a}\right)^m + \sum_{n=1}^{\infty} C_n\frac{I_m(\frac{n\pi r}{(d-h)})}{I_m(\frac{n\pi a}{(d-h)})}cos(\frac{n\pi z}{(d-h)}) \tag{24}$$

where C_n are unknown Fourier coefficients and I_m is the modified Bessel function of the first kind order m.

3.2.2. *Exterior domain*

The homogeneous solution of the exterior diffraction problem is given as:

$$\varphi_{3,h} = cos(k_n(z+d))\left[I_m(k_n r) - \frac{I'_m(k_n a)}{H'_m(k_n a)} H_m(k_0 r)\right] + D_0 \frac{H_m(k_0 r)}{H_m(k_0 a)} Z_0(z) + \sum_{n=1}^{\infty} D_n \frac{K_m(k_n r)}{K_m(k_n a)} Z_n(z) \quad (25)$$

where D_n are unknown Fourier coefficients. H_m is Hankel function, and K_m is the modified Bessel function of the second kind, both of order m.

3.3. Matching Conditions

In both the radiation and diffraction problem, the matching conditions represent the continuity of mass flux, pressure and normal velocity. The velocity potentials between interior and exterior domains are matched at the imaginary boundary $r = a$.

$$\phi^E = \phi^I, \ (r = a, -h \le z \le -d) \quad (26)$$

$$\frac{\partial \phi^E}{\partial r} = 0, \ (r = a, -h \le z \le 0) \quad (27)$$

$$\frac{\partial \phi^E}{\partial r} = \frac{\partial \phi^I}{\partial r}, \ (r = a, -d \le z \le -h) \quad (28)$$

The unknown Fourier coefficients C_n, D_n, C_{Rn}, D_{Rn} are solved using the matching conditions. The hydrodynamic coefficients are found by integrating the potential functions over their corresponding area. Detailed solution for this problem can be found in literature.

3.4. Validation of semi-analytic hydrodynamic coefficients using numerical NEMOH BEM

To validate the present method and its efficiency for use in the heterogeneous array optimization; the hydrodynamic coefficient of an array of two heaving semi-submerged devices having different sizes, as shown in Fig. 3 is computed. The radii are, $r = 5$ m,$R = 8$ m and draughts $h = 4$ m, $H = 7$ m. The hydrodynamic response is computed for frequency range, $\omega = 0.1 - 6\ rad/s$. The separation distance between the devices is $8r$. The constant water depth is $d = 50$ m and the incident wave-heading angle is 0^0 along the x-axis.

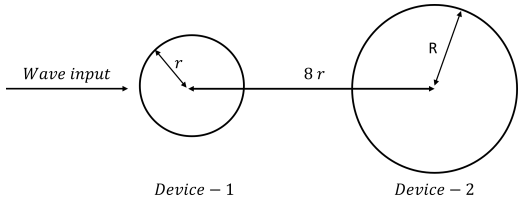

Figure 3: Layout of two floating vertical cylinders.

The heave exciting forces for device-1 and 2 is plotted presented in Fig. 4. The added mass coefficient and damping coefficient for corresponding devices are plotted in Figures 5 and 6, respectively. Plotted on the same figures are the hydrodynamic coefficients for the same devices as obtained from NEMOH BEM routine. The hydrodynamic coupling representing the off-diagonal terms in $\boldsymbol{A}$, $\boldsymbol{B_r}$ are presented in Figures 7 and 8. The figures show very good agreement between the numerical BEM and semi-analytic method. The small fluctuations observed at low frequencies often result from the scattered waves which is often not exactly captured by the semi-analytical method, similar behavious is observed in (Göteman et al., 2015; Yilmaz, 1998). The overall agreement is good.

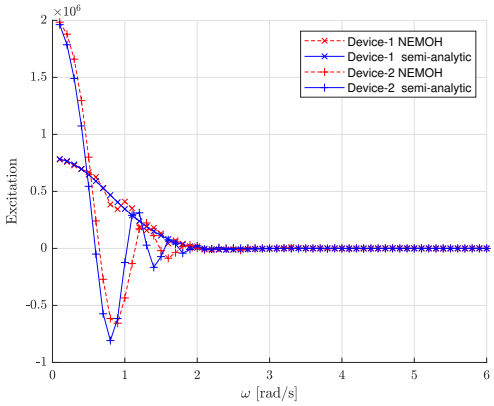

Figure 4: Heave wave-exciting forces on devices in the array.

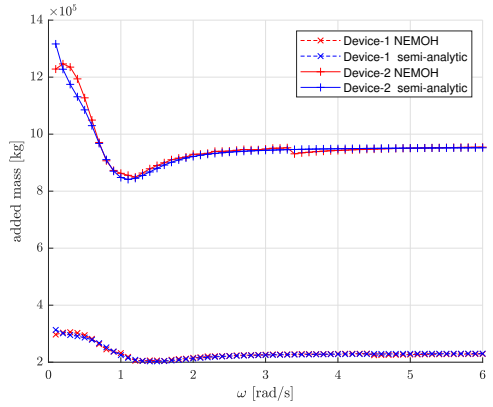

Figure 5: Added mass coefficients of the array.

4. Optimization problem formulation

In this section, the optimization problem will be formulated. In the first case, the optimized layout of arrays of 3, 5 and 7 devices from (Moarefdoost et al., 2017) presented in Fig. 9 is adapted as the layout of the array. In another case, a 3-device triangular layout is used. In all cases, the layouts are symmetric along the exciting wave direction (x-axis) and they all layout a device at the origin.

Genetic algorithm is chosen as the optimization algorithm. Genetic Algorithm is an adaptive meta-heuristic search algorithm classified as an evolutionary computing algorithm well documented in (Paulinas and Ušinskas, 2007;

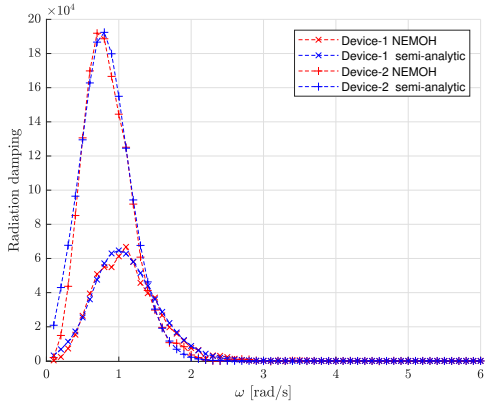

Figure 6: Damping coefficients of the arrays.

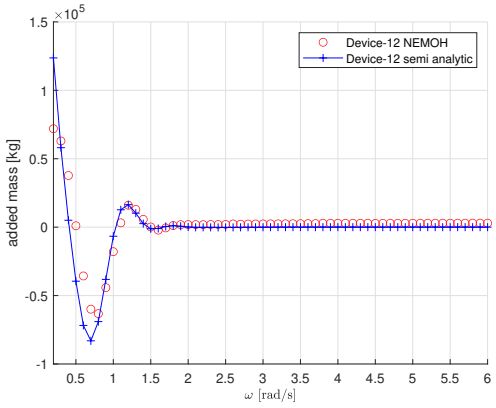

Figure 7: Added mass coupling between the devices in the array.

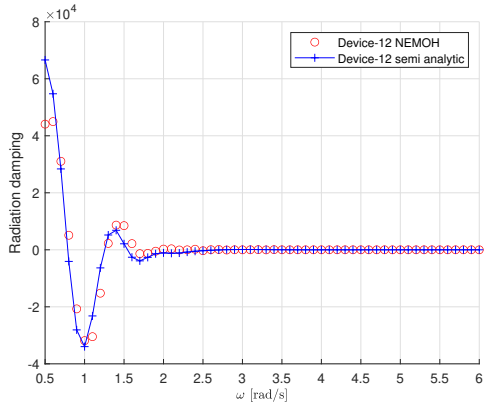

Figure 8: Damping coefficients coupling between the devices in the array.

Whitley, 1994; Houck, Joines and Kay, 1995) and many more references. Genetic algorithms have been used widely in wave energy converters optimization problems.

4.1. Parameter optimization of the dimensions of devices in a homogeneous array

In the current optimization problem, we want to determine the dimension of a WEC (radius and draught) that maximizes the positive inter-device interaction when placed

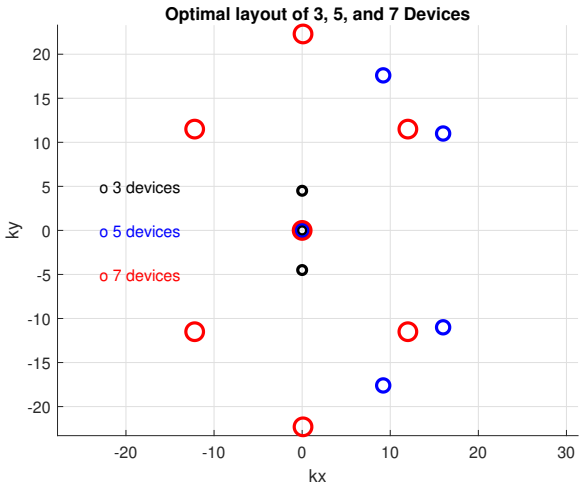

Figure 9: Optimal layout for 3, 5 and 7 devices from (Moaref-doost et al., 2017).

in the locations discussed in the previous section. The optimization objective remains the maximization of the q-factor:

$$\begin{aligned} q &= \frac{\boldsymbol{P}_{array}}{N\,\boldsymbol{P}_{isolated}} \\ s.t.\ R &\in [R_{min.}\ R_{max.}], \\ D &\in [D_{min.}\ D_{max.}]. \end{aligned} \tag{29}$$

The GA generated random population of radius and draught between the set upper bound and lower bound. The q-factor achieved by every member of the population is computed; constructive interaction means $q > 1$, else, it is destructive. The details of the optimization sequence is shown in Fig. 10. The best performing R and D are returned as the best dimension for the homogeneous N-devices for the specified wave condition and layout.

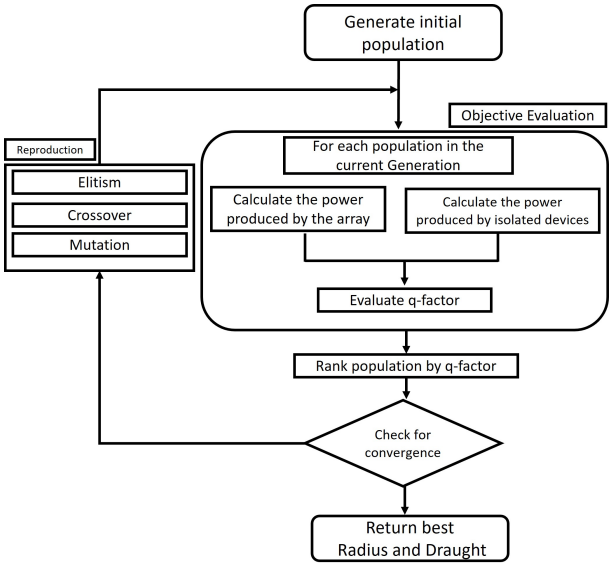

Figure 10: GA flowchart for size optimization of homogeneous array.

4.2. Optimization of heterogeneous WEC array

The first thing to make clear in the heterogeneous array optimization problem is that, the performance of the heterogeneous array is measured with respect to an optimized homogeneous array. The optimizer find the combination of devices of different dimensions located at the same location as the homogeneous array, subject to constraints on dimensions and total volume of the homogeneous array in consideration. In this problem, the q-factor would not be the performance measure as there would be no real comparison to the homogeneous array. For this reason, we present the p-factor:

$$\begin{aligned} p-factor &= \frac{\boldsymbol{P}_{heterogeneous}}{\boldsymbol{P}_{homogeneous}} \\ s.t.\ R_i &\in [R_{min}.\ R_{max.}], \\ D_i &\in [D_{min.}\ D_{max.}], \\ \forall\, i &= 1:N, \end{aligned} \tag{30}$$

T.V. of Het. array $= \pm\, 5\% \times$ **T.V. of Hom. array.**

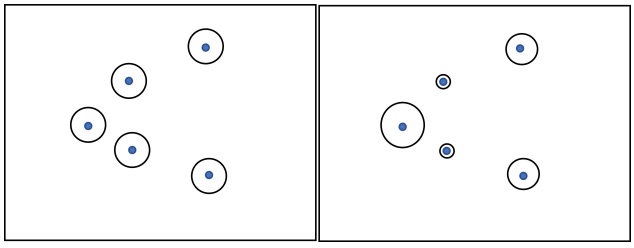

Figure 11: a) Homogeneous array (left), b) heterogeneous array (right).

where T.V. is an acronym for total volume. An illustration of the homogeneous and heterogeneous array is presented in in Fig. 11, the optimal radius and draught of the device in the homogeneous array will be found in the optimization problem section. 4.1. The power from this optimized array is the denominator of the p-factor from Eq. (30). The numerator of of the p-factor is the power from the array containing devices of different dimension as in Fig. 11. The total volume (T.V.) of the homogeneous devices is computed and used as the maximum volume constraint for the heterogeneous array optimization. Similar to the q-factor, when $p > 1$, this translates to a better performance by the heterogeneous array, otherwise, $p < 1$ means the heterogeneous optimization does not result in better performance. Theoretically, we expect p should not be less than 1; if there is no better performing heterogeneous solution, the size of the devices in the heterogeneous optimization should converge to the dimensions of the homogeneous array, thereby, $p = 1$. A flowchart of the heterogeneous array optimization is presented in Fig. 12.

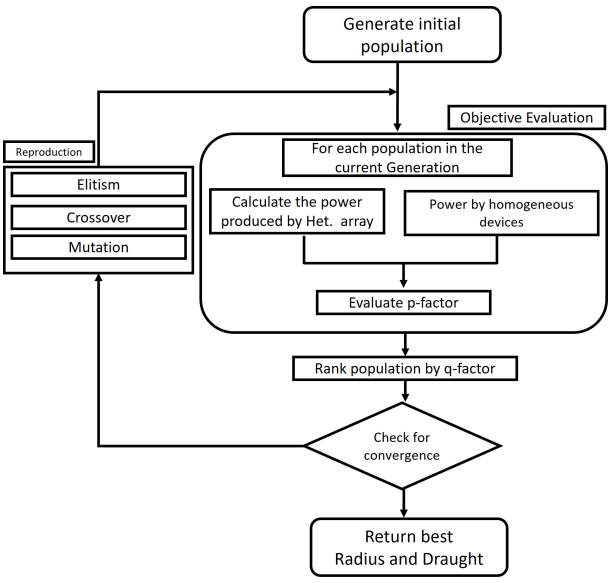

Figure 12: GA flowchart for heterogeneous array optimization.

5. Numerical Simulation Results

This section presents results from the homogeneous and heterogeneous array optimization for arrays containing 3,5 and 7 devices. In Section 5.1 and 5.2, the optimal layouts adapted from (Moarefdoost et al., 2017) are used the layout, while a random non-optimal layout is used in Section 5.3. The wave period and wave height at the deployment location are chosen as $T = 6.00$ s, wave height $H = 0.8222$ m. The time-domain dynamic model and PCBSB control discussed in Section 2 is implemented in the array optimization problem, the maximum limit of the control force of PTO units is set as $\Upsilon = 0.1 \times f_e(\omega)$ N. hydrodynamic coefficients are computed using the semi-analytic model presented in Section 3. The results presented in this section are from multiple runs of the optimization. The simulations are conducted in MATLAB.

5.1. Optimization of the dimensions of devices in a homogeneous array

The optimal radius and draught of the devices in the 3-device array is shown in Fig. 16. The upper and lower bound constraint of the optimization is as presented in Table 1. The optimized radius and draught are found to be $R = 7.22$ m, and $D = 5.81$ m, respectively. The optimal value of the dimensions is not close to the boundary of the constraint, indicating that the optimal solution is not out of the constraint domain. Constructive interference is maintained, with $q = 2.2332$. Similarly, the dimension for the 5 and 7 device array is presented in Fig. 14 and 15. The optimized dimension, interaction factor, and the total power from the optimized homogeneous array is documented in Table 2. The plots are scaled for a clearer presentation.

As expected, the average power from the array increases with increasing the number of devices. The variation of the dimensions is, however, not in the same order. The array of 3-device array has the largest R value and shortest D value. The smallest R value and longest D value is found to be the dimensions for 5 devices while the R,D values of the

Parameter	Unit	Lower Bound	Upper Bound
Radius	m	1	10
Draught	m	1	10

Table 1
Constraints on the optimization parameters.

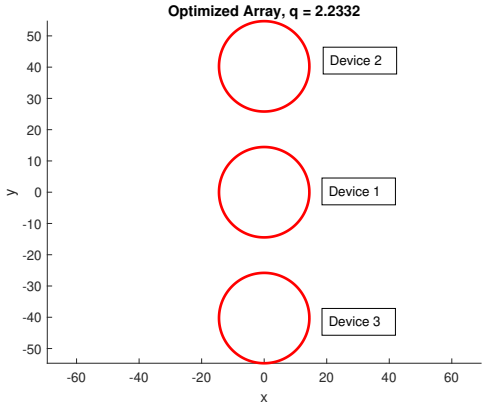

Figure 13: Optimized size for array of 3 devices.

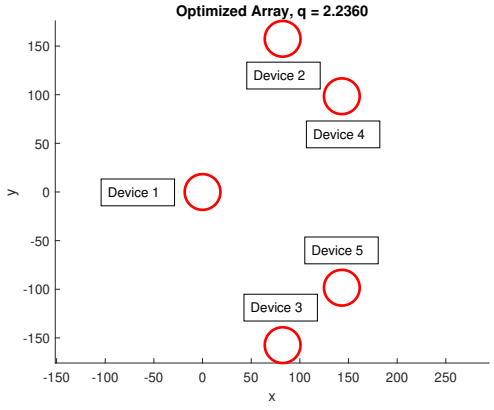

Figure 14: Optimized size for array of 5 devices.

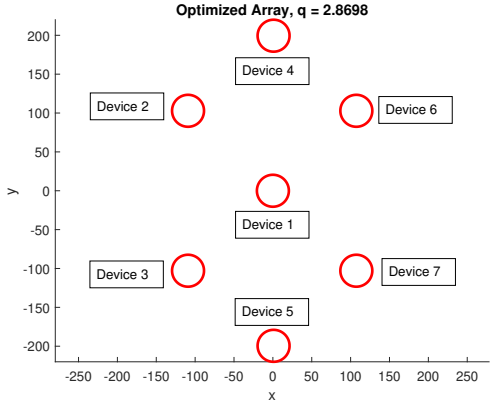

Figure 15: Optimized size for array of 7 devices.

N	R,D (m)	q	Power(kW)
3 devices	R = 7.22, D = 5.81	2.2332	1379.6
5 devices	R = 6.12, D = 6.59	2.2360	1747.8
7 devices	R = 6.85, D = 6.18	2.8698	3643.7

Table 2
The optimized dimension, q-factor and absorbed power from size optimization of the homogeneous arrays.

7-device array turns out to be the median dimensions on the table. The q-factors obtained for the optimized dimensions are all greater than 2, indicating very strong constructive interaction between the devices.

5.2. Optimization of the heterogeneous dimensions for buoys in an array

In this section, the optimized homogeneous array from section 5.1 is the basis for the heterogeneous array optimization. The optimizer will attempt to find an array containing devices with varying radii and draughts, achieving better performance than the optimized homogeneous array with the same number of devices and layout. The wave condition, and the constraints from the homogeneous optimization remain the same, with an additional constraint on the total volume of the heterogeneous array. The average power from the array, and the total volume of the optimized 3, 5, and 7 device array are inputs to the optimizer in this section. The result of the top 2 best performing arrays are plotted. It should be noted that the plots are scaled for clearer presentation of the results.

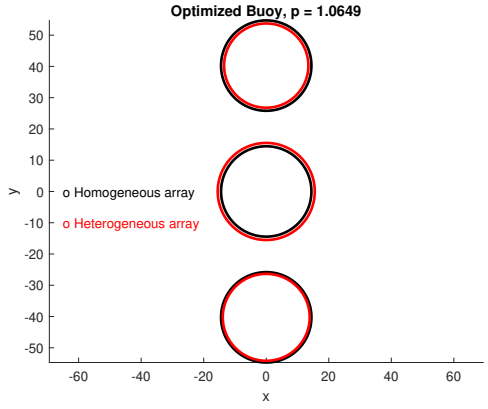

Figure 16: Optimized heterogeneous array of 3 devices.

For an array of 3 devices, it can be observed in Fig. 16 and 17 that the optimizer converges toward making the radius of device 1 bigger, while the draught is shortened when compared to the dimension of the homogeneous array. The optimal radii of devices 2 and 3 are found to be smaller than the radius of the homogeneous array. Overall, the optimized dimensions appear to converge towards being symmetric about the center device. An average performance improvement of 6.06% was achieved by the heterogeneous array over the homogeneous array The details of the resulting optimized dimensions are presented in Table 3.

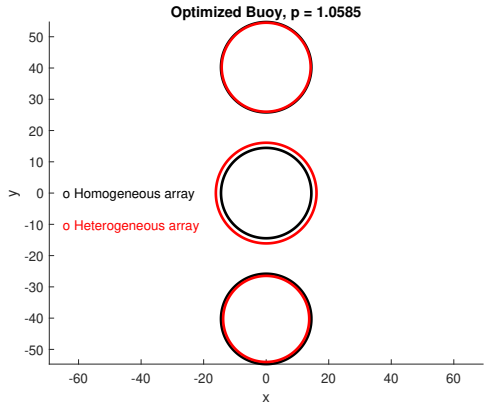

Figure 17: Optimized heterogeneous array of 3 devices.

No	R1	R2	R3	D1	D2	D3	p
1	8.04	6.81	7.19	5.24	5.88	5.78	1.0584
2	7.76	6.74	6.95	5.28	5.86	5.80	1.0649
3	8.04	7.12	6.89	5.24	5.75	5.89	1.0585

Table 3
3 device heterogeneous optimization run.

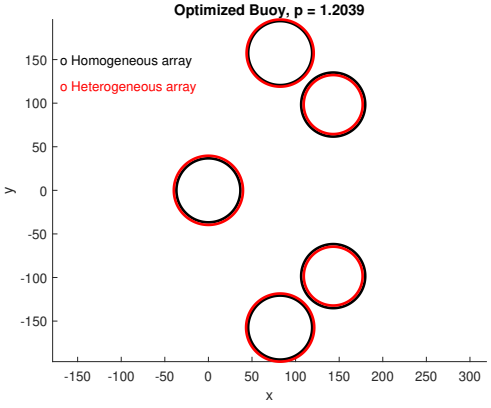

Figure 18: Optimized heterogeneous array of 5 devices.

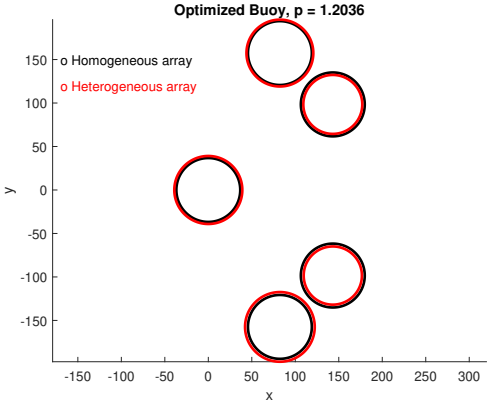

Figure 19: Optimized heterogeneous array of 5 devices.

The heterogeneous optimized dimension for the 5-device array is plotted in Fig. 18 and 19, the optimal solutions plots

No	R1	R2	R3	R4	R5	D1	D2	D3	D4	D5	p
1	6.52	6.40	6.70	5.68	5.56	5.86	5.93	5.85	6.61	6.55	1.2010
2	6.61	6.41	6.51	5.64	5.63	5.90	5.96	5.91	6.60	6.60	1.2039
3	6.52	6.40	6.67	5.65	5.58	5.91	5.94	5.85	6.59	6.61	1.2036

Table 4
5 device heterogeneous optimization run.

No	R1	R2	R3	R4	R5	R6	R7	D1	D2	D3	D4	D5	D6	D7	p
1	6.52	6.96	6.90	6.53	6.53	7.34	7.35	6.17	5.83	5.86	6.15	6.13	5.54	5.53	1.1035
2	6.70	6.86	6.90	6.35	6.36	7.51	7.47	6.12	5.95	5.93	6.21	6.21	5.53	5.54	1.0924
3	6.44	6.945	7.10	6.9	6.88	7.63	7.40	6.19	5.86	5.81	6.08	6.06	5.50	5.55	1.0954

Table 5
7 device heterogeneous optimization run.

are very similar. The heterogeneous devices are symmetric along the x-axis. The optimal radii of devices 1, 2 and 3 was found to be bigger than the homogeneous radius, while the radius of the trailing devices 4 and 5 are smaller than the homogeneous radius. A significant 20.02% average performance increase was attained by the heterogeneous array over the homogeneous array. The converged dimensions and p-factors are detailed in Table 4.

The optimized 7-device arrays are plotted in Fig. 20 and 21. As observed, the optimized heterogeneous dimensions also tend to converge towards being symmetric along the x-axis. In Fig. 20, the optimal radii of two leading devices 2 and 3 are found to be almost the same radius as the homogeneous array, the radii of devices 1, 4, and 5 located in the middle column are found to be smaller, while the radii of trailing devices 6 and 7 are found to be bigger than the homogeneous dimensions. In Fig. 21, the optimal radii of devices 2,3,4, and 5 were found to be very close to that of the homogeneous radius. Device-1, located at the center was found to be smaller, while the radii of the trailing devices 6 and 7 are bigger than the homogeneous radius. An average performance improvement of 9.71% was observed for heterogeneous array over the homogeneous array. The optimized heterogeneous dimensions and their performance is documented in Table 5.

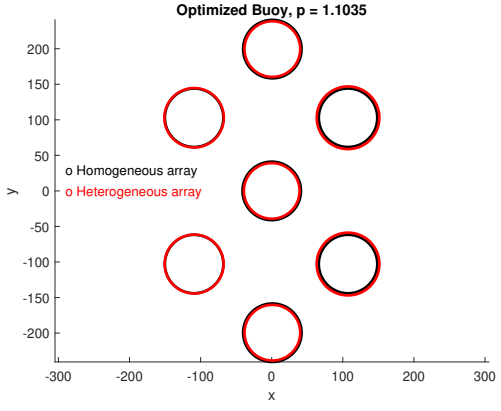

Figure 20: Optimized heterogeneous array of 7 devices.

Overall, better performance was achieved by using heterogeneous devices in the layout containing 3, 5 and 7 devices.

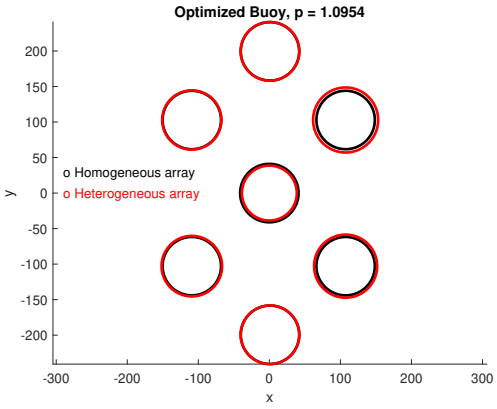

Figure 21: Optimized heterogeneous array of 7 devices.

No	R1	R2	R3	D1	D2	D3	p
1	4.37	3.94	3.82	6.47	7.21	7.21	1.7872
2	9.02	4.31	4.54	1.00	6.67	6.51	1.7620

Table 6
3 device heterogeneous optimization run.

5.3. Optimization of the homogeneous and heterogeneous arrays in random layout.

In this section, we adopt a generic triangular layout configuration, similar to the square and circular layout designs, the triangular layout is pretty common in literature. We ran homogeneous optimization to find the dimension of the device that has the best interaction in the layout, then heterogeneous optimization to find the better performing heterogeneous array. The objective function of the homogeneous and heterogeneous optimization remains as is in the previous sections. The optimal dimension obtained from the homogeneous optimization is $R = 3.69$ m and $D = 7.95$ m. The performance of the homogeneous array was, however, destructive with $q = 0.9953$.

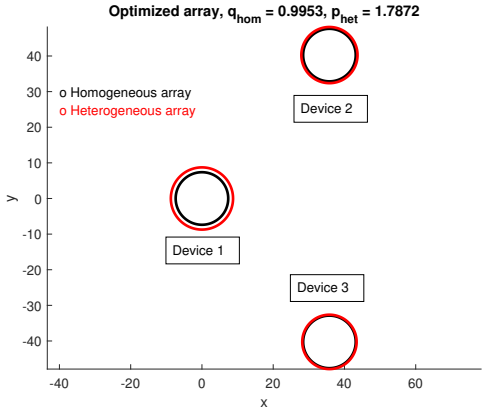

Figure 22: Optimized homogeneous and heterogeneous array of 3 devices.

The 2 best performing optimized dimensions of the homogeneous and heterogeneous optimization is plotted in Fig. 22 and 23. Due to the fact that the best q-factor of the homogeneous array is found to be < 1, with a lot of room for improvement by the heterogeneous array, and the p-factors are found to be significantly higher than 1. The optimized heterogeneous array is found to be symmetric along the wave direction. Optimized radii of all devices are found to be bigger than the homogeneous radius. An interesting result in Fig. 23 with a dramatically large optimized radius for the leading device-1; the radius becomes very close to the maximum radius and the draught at the minimum value. With an average performance improvement of 77.46% was observed for heterogeneous array over the homogeneous array, the major takeaway from this result is that; significantly greater improvement can be achieved by the heterogeneous array when the homogeneous array being considered is, for any reason, not achieving the optimal interaction between the devices in the array.

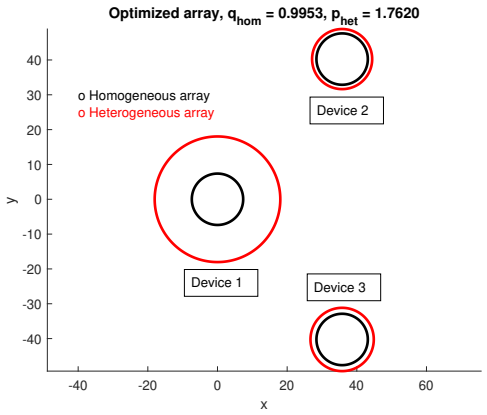

Figure 23: Optimized homogeneous and heterogeneous array of 3 devices.

6. Conclusion

In this work, we have investigated improving the performance of an array by allowing devices of different dimensions in the array. Two optimization problems were investigated, the first being parameter optimization of buoy dimensions that achieve the most constructive interference in an optimized layout. Heterogeneous array for the same optimal configuration was then investigated. Finally, we explore how heterogeneous arrays could significantly improve the performance of an array without optimal layout while constraining the total volume of the heterogeneous array to be the same as that of the homogeneous array within tolerance of $\pm 5\%$. In all simulations, the time-domain dynamic model coupled with an optical power-constrained Bang Singular Bang (PCBSB) control was used to compute the array's power to ensure the most realistic power results from the array. The hydrodynamic coefficients used as input to the dynamic model and control are computed using a semi-analytic approach, the efficiency of this semi-analytic approach in capturing inter-device hydrodynamic coupling is also demonstrated. Simulations showing the optimized

heterogeneous array converging toward a symmetric distribution and achieving better performance is presented in the results section. Overall, improved performance is possible when using heterogeneous arrays over homogeneous arrays.

CRediT authorship contribution statement

Habeebullah Abdulkadir: Methodology, Simulation, Initial draft of manuscript. **Ossama Abdelkhalik:** Conceptualization of this study, Methodology, Supervised research, Edited and reviewed manuscript.

References

Abdulkadir, H., Abdelkhalik, O., 2022. Optimal constrained control of wave energy converter arrays, in: 2022 American Control Conference (ACC), pp. 3100–3105. doi:10.23919/ACC53348.2022.9867173.

ANSYS, A., 2013. Version 15.0; ansys. Inc.: Canonsburg, PA, USA November 752.

Antonio, F.d.O., 2010. Wave energy utilization: A review of the technologies. Renewable and sustainable energy reviews 14, 899–918.

Babarit, A., 2010. Impact of long separating distances on the energy production of two interacting wave energy converters. Ocean Engineering 37, 718–729.

Babarit, A., Delhommeau, G., 2015. Theoretical and numerical aspects of the open source bem solver nemoh, in: 11th European Wave and Tidal Energy Conference (EWTEC2015).

Bacelli, G., Ringwood, J., 2013. Constrained control of arrays of wave energy devices. International Journal of Marine Energy 34, e53 – e69. URL: http://www.sciencedirect.com/science/article/pii/S2214166913000374, doi:http://dx.doi.org/10.1016/j.ijome.2013.11.011. special Issue Selected Papers - {EWTEC2013}.

Bozzi, S., Giassi, M., Miquel, A.M., Antonini, A., Bizzozero, F., Gruosso, G., Archetti, R., Passoni, G., 2017. Wave energy farm design in real wave climates: the italian offshore. Energy 122, 378–389.

Brekken, T.K., 2011. On model predictive control for a point absorber wave energy converter, in: 2011 IEEE Trondheim PowerTech, IEEE. pp. 1–8.

Budal, K., 1977. Theory for absorbtion of wave power by a system of interacting bodies. Journal of Ship Research 21, 248–253.

Child, B., Venugopal, V., 2010a. Optimal configurations of wave energy device arrays. Ocean Engineering 37, 1402–1417.

Child, B., Venugopal, V., 2010b. Optimal configurations of wave energy devices. Ocean Engineering 37, 1402–1417.

Cruz, J., 2007. Ocean wave energy: current status and future prespectives. Springer Science & Business Media.

Cummins, W., . The Impulse Response Function and Ship Motions. David W. Taylor Model Basin Report.

De Andrés, A., Guanche, R., Meneses, L., Vidal, C., Losada, I., 2014. Factors that influence array layout on wave energy farms. Ocean Engineering 82, 32–41.

Drew, B., Plummer, A., Sahinkaya, M.N., 2009. A review of wave energy converter technology. Proceedings of the Institution of Mechanical Engineers, Part A: Journal of Power and Energy 223, 887–902.

Falcão, A.F., Henriques, J.C., 2016. Oscillating-water-column wave energy converters and air turbines: A review. Renewable Energy 85, 1391–1424.

Falnes, J., 1980. Radiation impedance matrix and optimum power absorption for interacting oscillators in surface waves. Applied ocean research 2, 75–80.

Falnes, J., 1999. Wave-energy conversion through relative motion between two single-mode oscillating bodies. Journal of Offshore Mechanics and Arctic Engineering 121, 32–38. URL: http://link.aip.org/link/?JOM/121/32/1, doi:10.1115/1.2829552.

Falnes, J., Hals, J., 2012. Heaving buoys, point absorbers and arrays. Philosophical Transactions of the Royal Society of London A: Mathematical, Physical and Engineering Sciences 370, 246–277.

Göteman, M., Engström, J., Eriksson, M., Isberg, J., 2015. Optimizing wave energy parks with over 1000 interacting point-absorbers using an approximate analytical method. International Journal of Marine Energy 10, 113–126.

Hals, J., Falnes, J., Moan, T., 2011. Constrained optimal control of a heaving buoy wave-energy converter. Journal of Offshore Mechanics and Arctic Engineering 133.

Houck, C.R., Joines, J., Kay, M.G., 1995. A genetic algorithm for function optimization: a matlab implementation. Ncsu-ie tr 95, 1–10.

Kagemoto, H., Yue, D.K., 1993. Hydrodynamic interaction analyses of very large floating structures. Marine structures 6, 295–322.

Kofoed, J.P., Frigaard, P., Friis-Madsen, E., Sørensen, H.C., 2006. Prototype testing of the wave energy converter wave dragon. Renewable energy 31, 181–189.

Li, G., Weiss, G., Mueller, M., Townley, S., Belmont, M.R., 2012. Wave energy converter control by wave prediction and dynamic programming. Renewable Energy 48, 392 – 403. URL: http://www.sciencedirect.com/science/article/pii/S0960148112003163, doi:http://dx.doi.org/10.1016/j.renene.2012.05.003.

Lyu, J., Abdelkhalik, O., Gauchia, L., 2019. Optimization of dimensions and layout of an array of wave energy converters. Ocean Engineering 192, 106543.

Matsui, T., Tamaki, T., 1981. Hydrodynamic interaction between groups of vertical axisymmetric bodies floating in waves, in: International symposium on hydrodynamics in ocean engineering, pp. 817–836.

McIver, P., 2002. Wave interaction with arrays of structures. Applied Ocean Research 24, 121–126.

McNatt, J.C., Venugopal, V., Forehand, D., 2015. A novel method for deriving the diffraction transfer matrix and its application to multi-body interactions in water waves. Ocean Engineering 94, 173–185.

Moarefdoost, M.M., Snyder, L.V., Alnajjab, B., 2017. Layouts for ocean wave energy farms: Models, properties, and optimization. Omega 66, 185 – 194. URL: http://www.sciencedirect.com/science/article/pii/S0305048316303127, doi:https://doi.org/10.1016/j.omega.2016.06.004. new Research Frontiers in Sustainability.

Nagata, S., Toyota, K., Yasutaka, Y., Setoguchi, T., Kyozuka, Y., Masuda, Y., 2007. Experimental research on primary conversion of a floating owc "backward bent duct buoy", in: The Seventeenth International Offshore and Polar Engineering Conference, OnePetro.

Neshat, M., Alexander, B., Sergiienko, N., Wagner, M., 2019. A new insight into the position optimization of wave energy converters by a hybrid local search. arXiv preprint arXiv:1904.09599 .

Nyangchak, N., 2022. Emerging green industry toward net-zero economy: A systematic review. Journal of Cleaner Production , 134622.

de O. Falcao, A.F., 2010. Wave energy utilization: A review of the technologies. Renewable and Sustainable Energy Reviews 14, 899 – 918. URL: http://www.sciencedirect.com/science/article/pii/S1364032109002652, doi:http://dx.doi.org/10.1016/j.rser.2009.11.003.

Ohkusu, M., 1969. On the heaving motion of two circular cylinders on the surface of a fluid. Kyushu University, Reprinted from: Reports of Research Institute for Applied Mechanics, Kyushu University, Volume XVII, No. 58, 1969 .

Olabi, A., Abdelkareem, M.A., 2022. Renewable energy and climate change. Renewable and Sustainable Energy Reviews 158, 112111.

Pastor, J., Liu, Y., 2014. Frequency and time domain modeling and power output for a heaving point absorber wave energy converter. International Journal of Energy and Environmental Engineering 5, 1–13.

Paulinas, M., Ušinskas, A., 2007. A survey of genetic algorithms applications for image enhancement and segmentation. Information Technology and control 36.

Ruiz, P.M., Nava, V., Topper, M.B., Minguela, P.R., Ferri, F., Kofoed, J.P., 2017. Layout optimisation of wave energy converter arrays. Energies 10, 1262.

Sergiienko, N.Y., Neshat, M., da Silva, L.S., Alexander, B., Wagner, M., 2020. Design optimisation of a multi-mode wave energy converter, in: International Conference on Offshore Mechanics and Arctic Engineering, American Society of Mechanical Engineers. p. V009T09A039.

Siddorn, P., Taylor, R.E., 2008. Diffraction and independent radiation by an array of floating cylinders. Ocean Engineering 35, 1289–1303.

Snyder, L.V., Moarefdoost, M.M., et al., 2014. Layouts for ocean wave energy farms: Models, properties, and heuristic .

Thomas, G., Evans, D., 1981. Arrays of three-dimensional wave-energy absorbers. Journal of Fluid Mechanics 108, 67–88.

WAMIT User Manual, V., 2013. 7.0; wamit. Inc: Chestnut, MA, USA .

Whitley, D., 1994. A genetic algorithm tutorial. Statistics and computing 4, 65–85.

Wolgamot, H., Taylor, P., Taylor, R.E., 2012. The interaction factor and directionality in wave energy arrays. Ocean Engineering 47, 65–73.

Yilmaz, O., 1998. Hydrodynamic interactions of waves with group of truncated vertical cylinders. Journal of Waterway Port Coastal and Ocean Engineering 124, 272–280.

Zhongming, Z., Linong, L., Xiaona, Y., Wangqiang, Z., Wei, L., et al., 2021. Eia projects nearly 50% increase in world energy use by 2050, led by growth in renewables .

Zou, S., Abdelkhalik, O., Robinett, R., Bacelli, G., Wilson, D., 2017. Optimal control of wave energy converters. Renewable energy 103, 217–225.

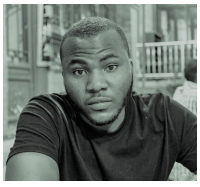

Habeebullah Abdulkadir received his MSc. degree in Aerospace Engineering at Beijing Institute of Technology, China in 2019. Since January 2021, he has been working toward his PhD degree at Iowa State University. His research interests is in ocean wave energy conversion.

Ossama Abdelkhalik is Associate Professor at Iowa State University. He received his PhD degree in Aerospace Engineering from Texas A&M University, and his BS and MS degrees from Cairo University in Egypt. Dr. Abdelkhalik's research is in the area of global optimization, dynamics, and control with applications to the wave energy conversion and space trajectory optimization. Dr. Abdelkhalik is Associate Fellow of AIAA and is associate editor of the AIAA Journal of Spacecraft and Rockets.